EFFECT OF ALUMINUM OXIDE ON THE STRUCTURE AND CONDUCTION BEHAVIORS OF SILVER BORATE GLASSES

G. El Damrawi[1*], A.M. Abdelghany[2] and H. Salaheldin[1]

[1]Glass research laboratory, Physics Department, Mansoura University, 35516 Mansoura, Egypt
[2]Spectroscopy Department, Physics Research Institute, National Research Centre, 33 El Behouth St, Dokki, 12311, Giza, Egypt

ABSTRACT. The current study focuses on glass preparation and characterization in the glass system of chemical formula xAl_2O_3 (35-x) $Ag_2O.65B_2O_3$ (0≤x≤35 mol%), where Ag_2O is replaced with Al_2O_3. To examine a wide range of both structure and morphology of the prepared glasses, nuclear magnetic resonance (NMR) of ^{27}Al nuclei, X-ray diffraction (XRD) spectroscopy, and transmission electron microscopy (TEM) are used. In Al_2O_3-rich glass, the well-formed AlO_6, AlO_5, and AlO_4 structural groups are the well-formed units. In samples of (20 and 30 mol % Al_2O_3), tetrahedral AlO_4 and traces from AlO_6 units could be detected. At lower concentrations of Al_2O_3 (10 mol%), the dominant forming unit is only AlO_4 groups containing non-bridging oxygen bonds (NBO). The XRD spectra confirm the amorphous nature of the glasses of Al_2O_3 <20 mol% while glasses of higher Al_2O_3 concentrations contain crystalline $Ag_2Al_2B_2O_7$ formed due to the higher oxygen packaging of the mixed AlO_5 and AlO_4 compared with that of glasses containing only AlO_4 species only. The morphology of crystalline units is confirmed from TEM to differ from that of an amorphous composition. The increase of activation energy and the hardness number of the glasses led to an increase in the durability of the investigated glasses.

KEY WORDS: Aluminum borate glass, NMR, Coordination of aluminum atom, Conductivity, Crystallization process

INTRODUCTION

In recent decades, glass or glass-ceramics containing Al_2O_3, such as Al_2O_3-B_2O_3, Al_2O_3-SiO_2, or Al_2O_3-B_2O_3-SiO_2, and Al_2O_3-P_2O_5 systems, have gotten a lot of attention [1-4]. This is because the presence Al_2O_3 can form interconnected bonds in glass systems, leading to an improvement in the chemical stability [5] and good mechanical properties [6, 7]. Physical properties of Al_2O_3-containing glasses, such as micro-hardness, conductivity, and chemical durability, are strongly linked to their Al coordination, which changes from six (AlO_6) to five (AlO_5) to four (AlO_4) coordination [7-10]. Then, for adjustments of the structure to get appropriate physical properties, it is important to control both the boron and aluminum coordinations in the investigated glasses.

The relation between adding network modifiers and changing in both boron and aluminum coordination had been documented in earlier reports [9, 11]. Increasing the molar ratio of modifier oxide to aluminum oxide should lower or suppress the concentration of higher coordinated Al species such as AlO_6 and AlO_5 in glasses. Reverse behavior was identified with increasing Al_2O_3 concentration in the glass network since higher-coordinated AlO_6 and AlO_5 can simply be formed because their cationic field strength is sufficiently large.

Recently, there are some available studies on alumina-based glasses and glass ceramics but little research attention has been paid to crystalline Ag_2O-Al_2O_3-B_2O_3 nano-composites. Studies concerning this issue are our main aim. The addition of Ag_2O to aluminum borate glasses can expand the glass formation region and generate the intended amounts of AlO_6 beside AlO_5, proportional to the ratio of Al_2O_3 to Ag_2O. In addition, at high Al_2O_3/Ag_2O_3 ratios, crystalline structural units can be formed in the range of nanoscale. Al_2O_3 oxide reinforced crystallized glasses [12-15] give the material a good advantage to be used as compatible dental fillers to enhance the hardness and other mechanical properties of dental material [12-14].

_____

Borate glasses containing silver, strontium, zinc, and/or cerium oxides can simply exhibit good compatibility with tissues and support cell proliferation [15-17]. But there is a problem in the case of releasing a high amount of boron ions during the dissolution process which may become toxic. To solve such a problem, mixing B_2O_3 with an additional glass former such as P_2O_5, SiO_2 or Al_2O_3 can regulate the process of ion release in the solution and prevent the toxicity to be performed. The mixed ion effect can also optimize the dissolution and boron release rate. Therefore, our aim in this work is to study the effect of mixing specific concentrations from Al_2O_3 with B_2O_3 in silver borate glasses. The Al_2O_3 can enhance the hardness and toughness of the glass and makes the material durable against corrosion. The Ag, as well as Cu ions, are known to promote the proliferation of endothelial cells, which are important processes for wound healing. In addition, Ag^+ ions in glasses have a good ability to be used as antibacterial agents giving the mixed former glasses more advantages for biomedical applications [18]. The present studies can also be extended to determine the electrical conduction mechanisms.

EXPERIMENTAL

Preparation of glasses

The chemically pure $AgNO_3$, H_3BO_3, and Al_2O_3 were used as starting materials that produce Ag_2O, B_2O_3, and Al_2O_3 respectively within the glass matrix. Stoichiometric powders were carefully mixed and heated in a platinum crucible to about 350 °C for 1h to get rid of nitrate and water. The temperature was then raised to about 1340-1450 °C depending on the glass composition. Obtained melt occasionally swirled several times to obtain bubble-free samples. Subsequently, melts were quenched on a metal plate that was pre-heated to 350 ºC to avoid cracking and thermal stresses. The resulting glasses had formulations of xAl$_2$O$_3$.(35-x) Ag$_2$O.65 B$_2$O$_3$ (x = 0-35 mol%). Sample nomination and composition were listed in Table 1.

Table 1. Sample nomination and composition.

Sample	Al$_2$O$_3$	Ag$_2$O	B$_2$O$_3$
0	0	35	65
10	10	25	65
15	15	20	65
20	20	15	65
25	25	10	65
35	35	0	65

Measurements

X-Ray diffraction measurements are carried out with a Shimadzu X-ray diffractometer (Dx-30, Metallurgy institute, El Tebbin-Cairo). The peak position and intensity values have been used to identify the type of material phases which were compared with patterns in the international powder diffraction file (PDF) database compiled by the joint committee for powder diffraction standards (JCPDS). NMR measurements were carried out at ambient temperature on a JEOL RESONANCE GSX-500 spectrometer operating at a high external magnetic field (11.747 T). ^{27}Al NMR spectra were measured at the resonance frequency of 130.2 MHz, using a 3.2 mm MAS NMR probe operated at a rotor frequency of 15 kHz. Typical pulse lengths were 2.5 μs and 60 seconds delay time was sufficient to enable relaxation. Spectra are referenced to Al(NO$_3$)$_3$ (0 ppm). ^{27}Al spectra were fit with Delta NMR software, version 5.04 (Japan) has been used for NMR analysis, simulation, and integration of the area under each species peak.

Electrical conductivity was measured for polished parallel surface samples adopting a sandwich arrangement using silver electrodes via Keithley 6517B electrometer. Resistance was measured as a function of reciprocal temperature with a precision of ±5% resulting in ±0.025 eV deviation in the estimated activation energy. The hardness of the specimens was determined using a digital Vickers microscope model (FM-7, Future-Tech Corporation, Kawasaki-Japan). The Vickers's hardness (H_V) test was performed under 50 g load and 15 s dwell time. The sample surface was polished, twelve indentations were performed on the surface of each specimen at ambient room temperature and the average value of the diagonal was used to calculate H_V.

RESULTS AND DISCUSSION

XRD and TEM-EDP

The formation of the crystalline aluminum-borate separated phases in some of the investigating compositions is very important in the broad field of applications. The ordered species from $Ag_2Al_2B_2O7$ [18] would play a good role in the improvement of hardness and compactness of the material network and consequently enhance its corrosion resistance. In addition, both boron and silver ions impeded in these crystalline phases play the role of antibacterial species. The formation of different types of B-O-Al, and Al-O-Al bonds in the network plays role in the enhancement of material properties. The bond types and their concentration in different phases can be documented utilizing both XRD pattern and NMR spectroscopy.
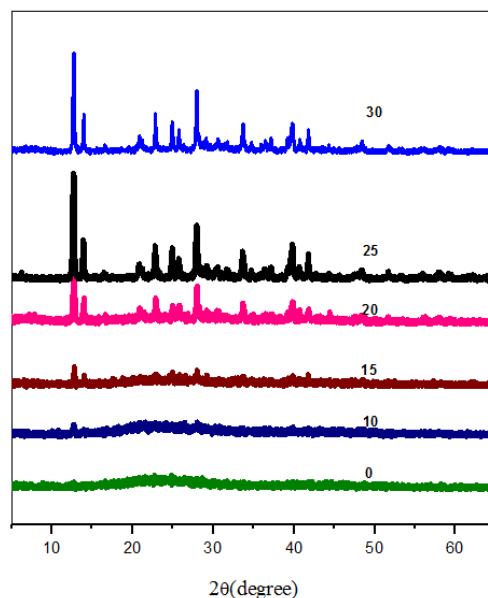

Figure 1. X-Ray diffraction spectra of some glasses.

XRD spectra (Figure 1) showed a structural change when Al_2O_3 is added to the Ag_2O-B_2O_3 network. The amorphous structure is the dominant type in the composition of up to 20 mol% Al_2O_3. The formation of crystalline $Ag_2Al_2B_2O_7$ phase is confirmed upon more additions of Al_2O_3. Increasing crystallinity of the Al_2O_3-rich glasses is accompanied by decreasing the rate of

transformation of BO_3 units to BO_4 groups leading to a decrease in the fraction of tetrahedral boron (N_4) [19-21]. Majority of silver oxide are consumed to modify Al_2O_3 forming groups (AlO_4) while the rest are used to modify B_2O_3 to form BO_4 tetrahedral units. The shortage in Ag_2O concentration upon Al_2O_3 replacement forces some of Al_2O_3 to enter as AlO_6 to compensate for the electronegativity around the well-formed structural units. Thus the introduction of Al_2O_3 into the borate matrix produces not only Al-O-Al-O-B bonds but also gives rise to an increase in the tendency to crystallization as is shown in Figure 1.

The results based on XRD is agreed to some extent with that obtained from TEM micrographs presented in Figures (2 and 3). As is shown from the figures, different species of different morphologies are simply shown. The electron diffraction pattern of this composition confirms the formation of the crystalline structure of the distributed species. On the other hand, the homogenous morphology with amorphous EDP is seen for a glass of lower Al_2O_3 concentration.
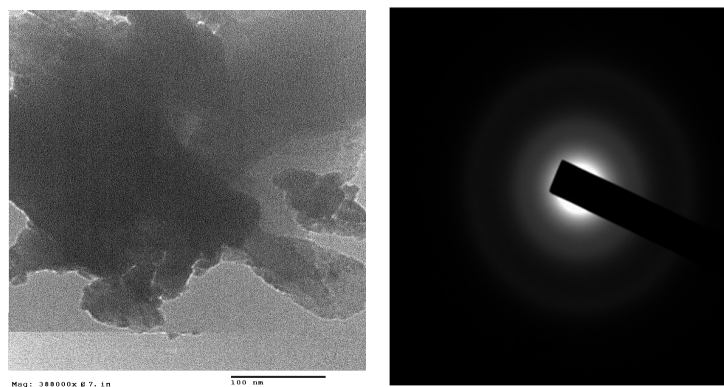

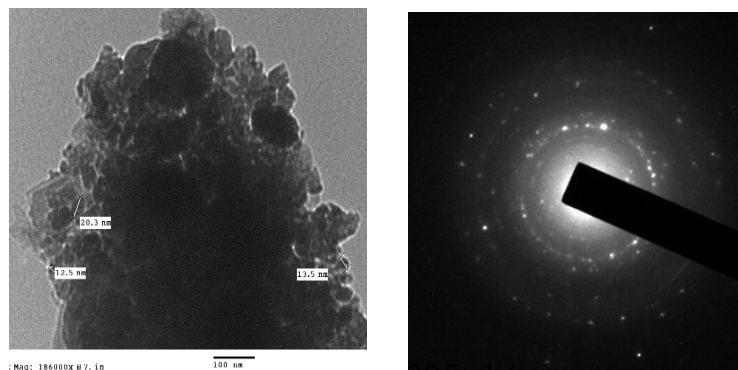Figure 2. TEM –EDP for a glass containing 15 mol% Al_2O_3.

Figure 3. TEM-EDP for a glass containing 30 mol% Al_2O_3.

Electrical conductivity

It is also important in this work to study the electrical properties of the investigated glasses. This is because to apply such material in the field of bio applications, its ability to conduct or resist current should be determined. A trial will be done to correlate the changes of both conductivity

and activation energy for ionic conduction with the structural changes detected by NMR spectroscopy upon replacing Ag_2O with Al_2O_3. At first, it can be assumed that Ag^+ ions related to the borate matrix are the predominant contributor to the conduction mechanism [22]

The studied glasses show a linear dependence of the logarithm of conductivity (log σ_{200}) with reciprocal of absolute temperature (1/T), Figure 4. This behavior is a feature of the ionic conduction process that can be described by the Arrhenius relation. Figure (5) shows that there is a fast change in both log σ_{200} and E with increasing Al_2O_3 contents. The result reveals that conductivity decreases by about six orders of magnitude upon replacing 30 mol% Ag_2O with Al_2O_3. The remarkable change in conductivity is accompanied by an increase of E from 1.2 eV to 0.51 eV.
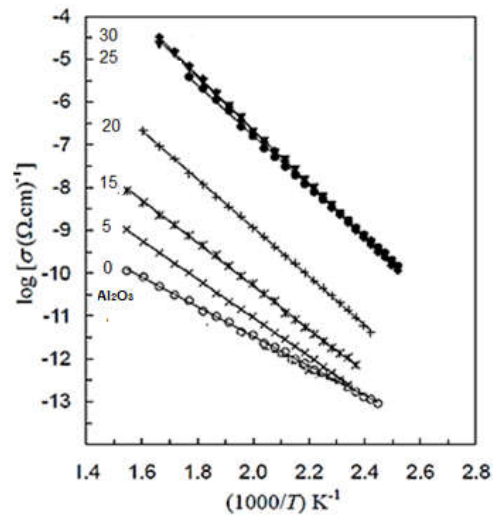

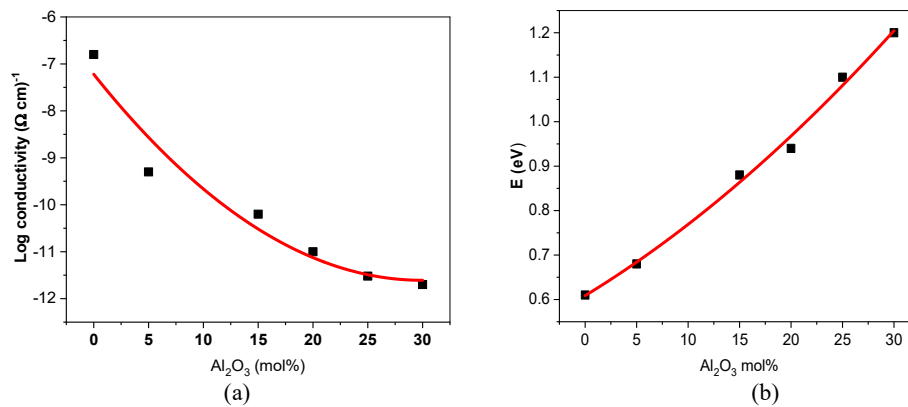Figure 4. Logarithm of conductivity (log σ) with reciprocal of absolute temperature (1000/T).

(a)   (b)

Figure 5. Changes in log σ_{200} and E with increasing Al_2O_3 contents.

The change of the Vickers hardness (H_v) with the Al_2O_3 content is shown in Figure 6. It can be seen that the hardness number increases with increasing Al_2O_3 content and there is a large

increase in the hardness value of the investigated system from about 2.3 to 4 GP as aluminum oxide content increases from 0 to 30 mol%. It is known that the increase in hardness is related to the increase in the rigidity of glass [23, 24]. These results are consistent with the increase in activation energy for conduction (Figure 5), the increase of both Hv and E_a indicated that the addition of Al_2O_3 created some units from five and six coordinated aluminum species. In addition, the relative concentration of three coordinated boron is also increased at expense of the four coordinated one. The presence of such units plays the role of strengthening the glass which may be reflected in the increasing behavior between the hardness number and Al_2O_3 content.
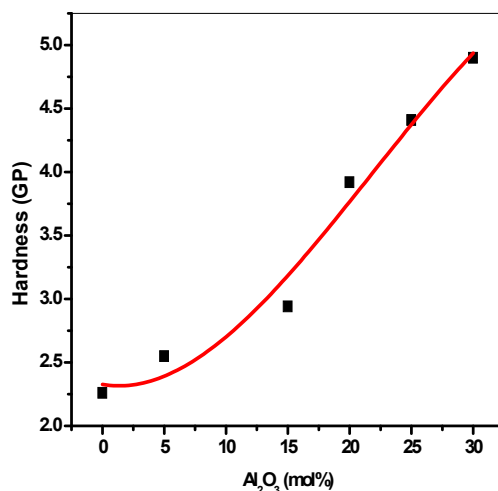

Figure 6. Variation of Vickers hardness number with increasing Al_2O_3 content.

Table (2) lists the estimated values of Electrical conductivity atspecific temperature (σ_{200}), activation energy in electron volts (eV) and Vicker hardness number (GP) of the studied samples.

Table 2.Electrical conductivity, activation energy and Vicker hardness number of the studied samples.

Sample	$\log\sigma_{200}$	E_a (eV)	Hv (GP)
0	-6.85	0.60	2.27
10	-9.22	0.68	2.53
15	-10.24	0.87	2.94
20	-10.95	0.93	3.95
25	-11.40	1.12	4.48
35	-11.55	1.21	4.87

^{27}Al NMR investigation

To understand the changes in the NMR spectra of the aluminate structural species, the role of Al_2O_3 must be firstly determined. For instance, the addition of Al_2O_3 to silicate or borosilicate glasses requires charge compensation which can be achieved by either depolymerization of the silicate network or the formation of AlO_6. At a high Al/Si ratio (greater than 1), the tetrahedral ($AlO_{4/2}$) is avoided to be linked together [25, 26] and as a result AlO_6 octahedral must be present in the form $(AlO_{6/2})^{3-}$. The situation is different to a great extent in Al_2O_3 borate glasses. Since most of Al_2O_3 would suppress the continued formation of BO_4 [27]. This is because Al_2O_3 enters

as a glass former (AlO$_4$) which is compensated with a modifier or with octahedral aluminum. Then not all the modifiers can consume in boron transformation but the main portion from Ag$_2$O can be used to form AlO$_4$ units as network former species.

Figure 7 represents ^{27}Al NMR spectra of three different compositions of the studied glasses. An intense ^{27}Al NMR resonance of chemical shift at about 55, 51, and 44 ppm arising from Al(4) was seen for glasses containing 10, 20, and 30 mol% Al$_2$O$_3$ respectively. This figure demonstrates that in every composition the main portion of the aluminum is acting principally as a network-former (AlO$_4$) species. Indeed there was a broad spectral peak which evidenced that a little of Al$_2$O$_3$ enters as Al(6) (small peak at about 16 ppm) in glasses of 20 and 30 mol%Al$_2$O$_3$. Similarly, the appearance of the Al(5) resonance only as a shoulder indicates a rather low concentration of this structural type within the glass. The distortions of the peak that represents AlO$_4$ resonance may be considered due to the effect of second-order quadrupolar interactions due to the presence of even low concentrations from AlO$_5$ structural units within the glass [28]. This consideration can be more evident from the analysis of the experimental spectra by the deconvolution process Figures (8.a-c). The resonance was found to have a contribution to the observed shoulder which can represent AlO$_5$ at about 35 and 40 ppm, Figures (8.b, c). Accurate integration of the NMR spectrum to give precise information concerning the relative amount of these structural elements was possible owing to the separation of the spectra into their component bands. The analyzed broad peak around 16 ppm (figures 8. a and b) represents AlO$_6$ octahedral units where such species (AlO$_6$) is expected to be formed to avoid two Al(4) bonding [28, 29].
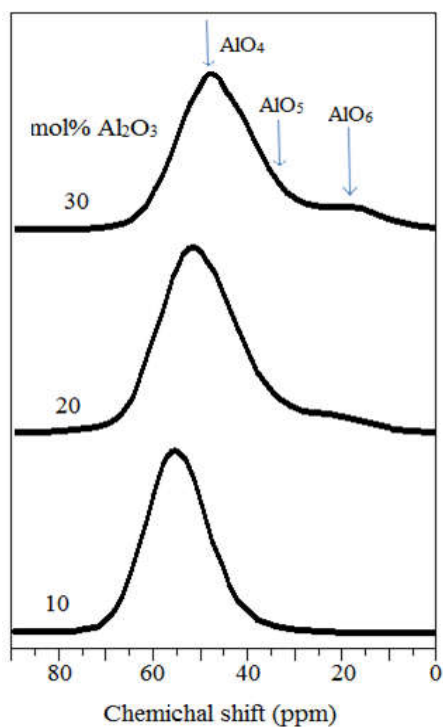

Figure 7. ^{27}Al MAS NMR spectra of silver borate glass containing 10, 20, and 30 mol% Al$_2$O$_3$.
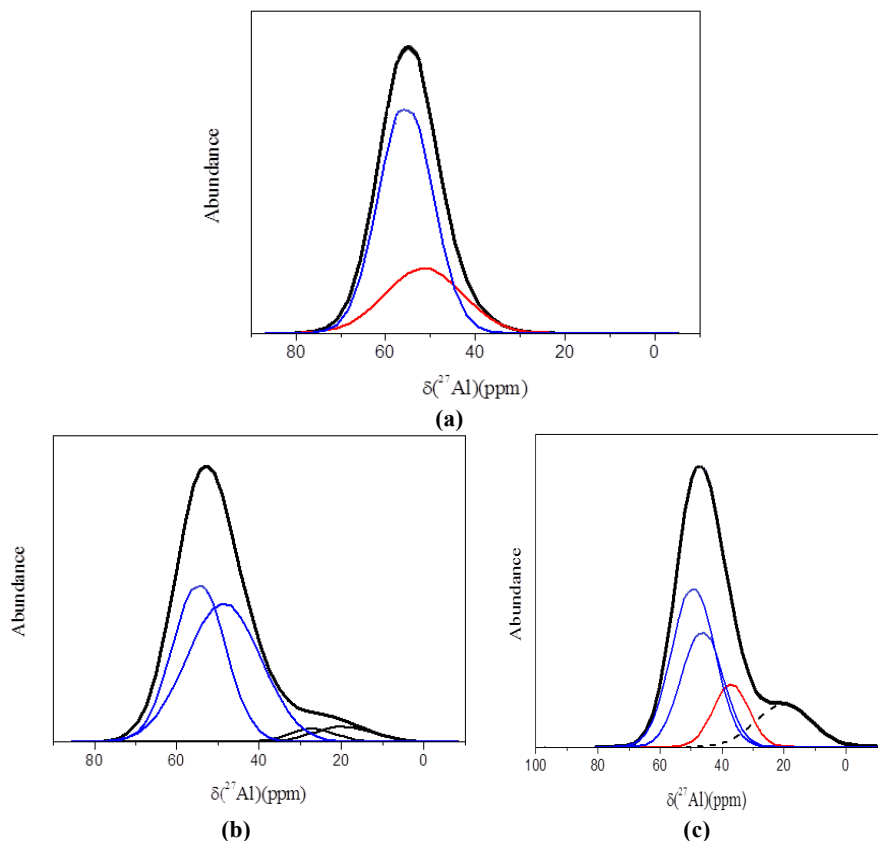
(a)

(b)

(c)

Figure 8a-c. Peak separation and integration for a glass containing 10, 20 and 30 mol%.

The NMR data therefore strongly suggest that adding Al_2O_3 changes the microstructure of the glass network. For instance, in the high Al/Ag ratio (>1), both Al(4) and Al(6) are significantly formed. But at lower Al/Ag ratios, only AlO_4 units are considered the main structural species representing the aluminate structure. Given that the excess aluminum can be consumed in constructing a regular silver borate phase containing aluminate species. This would imply that the glass with high alumina content is not homogenous. This result is in a good agreement with the TEM results presented in Figure 3 to some extent. As is shown from this figure different species of different morphology are seen (The electron diffraction pattern of this composition confirms the formation of the crystalline structure of the distributed species. On the other hand, the homogenous morphology with amorphous EDP is seen for a glass of lower Al_2O_3 concentration Figure 2.

CONCLUSION

The structure of silver aluminoborate (AgAlB) glasses containing a high concentration of Al_2O_3 (30 mol%) were studied by X-Ray diffraction, TEM microscopy, and ^{27}Al nuclear magnetic resonance (NMR) spectroscopy. The effects of replacing Ag_2O with AlO_3 content on the structure of the AgAlB glasses were evaluated. Al^{3+} ion enters into the glass structure mainly in fourfold

coordination, forming $(AlO_{4/2})^-$ tetrahedral. A small amount of Al^{3+} is found in fivefold and six-fold coordination. Al_2O_3 acts as network formers producing more bridging oxygen atoms with BO_3 units. The exchange of Ag_2O with Al_2O_3 decreases the conductivity and increases the activation energy for ionic conduction. The hardness of the studied glasses is improved with increasing Al_2O_3 content.

REFERENCES

1. Okada, G.; Shinozaki, K.; Komatsu, T.; Kawano, N.; Kawaguchi, N.; Yanagida, T. Tb^{3+}-doped BaF_2-Al_2O_3-B_2O_3 glass and glass-ceramic for radiation measurements. *J. Non. Cryst. Solids* **2018,** 501, 111-115.
2. Tarafder, A.; Molla, A.R.; Mukhopadhyay, S.; Karmakar, B. Fabrication and enhanced photoluminescence properties of Sm^{3+}-doped $ZnO–Al_2O_3–B_2O_3–SiO_2$ glass derived willemite glass–ceramic nanocomposites. *Opt. Mater.* **2014**, 36, 1463-1470.
3. Fabris, D.C.N.; Polla, M.B.; Acordi, J.; Luza, A.L.; Bernardin, A.M.; De Noni Jr, A.; Montedo, O.R.K. Effect of $MgO\cdot Al_2O_3\cdot SiO_2$ glass-ceramic as sintering aid on properties of alumina armors. *Mater. Sci. Eng. A* **2020**, 781, 139237.
4. Abdelghany, A.M.; Rammah, Y.S. Transparent alumino lithium borate glass-ceramics: synthesis, structure and gamma-ray shielding attitude. *J. Inorg. Organomet. Polym. Mater* **2021**, 31, 2560-2568.
5. Pershina, S.V.; Il'ina, E.A.; Druzhinin, K.V.; Farlenkov, A.S. Effect of $Li_2O–Al_2O_3–GeO_2–P_2O_5$ glass crystallization on stability versus molten lithium. *J. Non. Cryst. Solids* **2020**, 527, 119708.
6. Hou, Y.; Cheng, J.; Kang, J.; Yuan, J.; Cui, J. Structure, glass stability and rheological properties of $Na_2O–CaO–Al_2O_3–SiO_2$ glasses doped with Y_2O_3. *Ceram. - Silik* **2018**, 62, 173-180.
7. Souissi, F.Z.; Ettoumi, H.; Barré, M.; Toumi, M. Preparation and electrical conductivity of potassium phosphate glasses containing Al_2O_3. *J. Non. Cryst. Solids* **2018**, 481, 585-589.
8. Delaye, J.M.; Le Gac, A.; Macaluso, S.; Angeli, F.; Lodesani, F.; Charpentier, T.; Peuget, S. Investigation of alumino-silicate glasses by coupling experiments and simulations: Part I-Structures. *J. Non. Cryst. Solids* **2021**, 567, 120936.
9. Zhang, R.; Wang, Z.; Meng, Y.; Jiao, S.; Jia, J.; Min.; Y. Liu, C. Quantitative insight into aluminium structures in $CaO–Al_2O_3–SiO_2$ system via Raman and ^{27}Al MAS-NMR spectroscopies. *J. Non. Cryst. Solids* **2021**, 573, 121116.
10. Feng, X.; Yao, W.; Li, J. Effect of B_2O_3 on the structure of CaO-Al_2O_3-B_2O_3 ternary melts: A molecular dynamics simulation. *J. Non. Cryst. Solids* **2021**, 574, 121141.
11. Singh, H.; Shu, Q.; King. G.; Liang, Z.; Wang, Z.; Cao, W.; Huttula, M. Fabritius, T. Structure and viscosity of $CaO–Al_2O_3–B_2O_3–BaO$ slags with varying mass ratio of BaO to CaO. *J. Am. Ceram. Soc.* **2021**, 104, 4505-4517.
12. El-Damrawi, G.; Hassan, A.K.; Shahboub, A. Characteristic studies on Ag_2O-Al_2O_3-P_2O_5 glasses and glass ceramics. *Mater. Sci. Eng. B* **2021**, 264, 114957.
13. Kato, T.; Shiratori, D.; Iwao, M.; Takase, H.; Nakauchi, D.; Kawaguchi, N.; Yanagida, T. Ag concentration dependence of build-up effect of radio-photoluminescence in Ag-doped $P_2O_5–Al_2O_3–Na_2O–SiO_2$. *Sens. Mater.* **2021**, 33, 2163-2169.
14. Kato, K.; Hayakawa, T.; Kasuya, Y.; Thomas, P. Influence of Al_2O_3 incorporation on the third-order nonlinear optical properties of $Ag_2O–TeO_2$ glasses. *J. Non. Cryst. Solids* **2016**, 431, 97-102.
15. Liu, X.; Xie, Z.; Zhang, C.; Pan, H.; Rahaman, M.N.; Zhang, X.; Fu, Q.; Huang, W. Bioactive borate glass scaffolds: in vitro and in vivo evaluation for use as a drug delivery system in the treatment of bone infection. *J. Mater. Sci. Mater. Med* **2010**, 21, 575-582.
16. Abdelghany, A.M. Novel method for early investigation of bioactivity in different borate bio-

glasses. *Spectrochim. Acta A Mol. Biomol. Spectrosc.* **2013**, 100, 120-126.

17. Abdelghany, A.M.; El Batal, H.A.; Ezz El Din.; F.M. Bone bonding ability behavior of some ternary borate glasses by immersion in sodium phosphate solution. *Ceram. Int.* **2012**, 38, 1105-1113.

18. Hum, J.; Boccaccini, A.R. Bioactive glasses as carriers for bioactive molecules and therapeutic drugs: A review. *J. Mater. Sci. Mater. Med.* **2012**, 23, 2317-2333.

19. Kurajica, S.; Šipušić, J.; Zupancic, M.; Brautović, I.; Albrecht, M. ZnO-Al_2O_3-SiO_2 glass ceramics: Influence of composition on crystal phases, crystallite size and appearance. *J. Non. Cryst. Solids* **2021**, 553, 120481.

20. El-Damrawi, G.; Abdelghany, A.M.; Hassan, A.K.; Faroun, B. Conductivity and morphological studies on iron borosilicate glasses. *J. Non. Cryst. Solids* **2020**, 545, 120233.

21. El-Damrawi, G.; Abdelghany, A.M.; Hassan, A.K.; Faroun, B. Effect of BO_4 and FeO_4 structural units on conduction mechanism of iron borosilicate glasses. *Silicon* **2021**, 13, 4025-4031.

22. Okasha, A.; Marzouk, S.Y.; Hammad, A.H.; Abdelghany, A.M. Optical character inquest of cobalt containing fluoroborate glass. *Optik* **2017**, 142, 125-133.

23. Bauchy, M.; Qomi, M.J.A.; Bichara, C.; Ulm, F.J.; Pellenq, R.J.M. Rigidity transition in materials: hardness is driven by weak atomic constraints. *Phys. Rev. Lett.* **2015**, 114, 125502.

24. Liu, P.; Januchta, K.; Jensen, L.R.; Bauchy, M.; Smedskjaer, M.M. Competitive effects of free volume, rigidity, and self-adaptivity on indentation response of silicoaluminoborate glasses. *J. Am. Ceram. Soc.* **2020**, 103, 944-954.

25. Abd El-Moneim, A.; Youssof, I.M.; Abd El-Latif, L. Structural role of RO and Al_2O_3 in borate glasses using an ultrasonic technique. *Acta Mater.* **2006**, 54, 3811-3819.

26. Bruns, S.; Uesbeck, T.; Weil, D.; Möncke, D.; Van Wüllen, L.; Durst, K.; De Ligny, D. Influence of Al_2O_3 addition on structure and mechanical properties of borosilicate glasses. *Front. Mater.* **2020**, 7, 189.

27. Singh, G.P.; Kaur, S.; Kaur. P.; Singh, D.P. Modification in structural and optical properties of ZnO, CeO_2 doped Al_2O_3–PbO–B_2O_3 glasses. *Phys. B: Condens. Matter* **2012**, 407, 1250-1255.

28. Schaller, T.; Stebbins, J.F. The structural role of lanthanum and yttrium in aluminosilicate glasses: A ^{27}Al and ^{17}O MAS NMR study. *J. Phys. Chem. B* **1998**, 102, 10690-10697.

29. Du, W.F.; Kuraoka, K.; Akai, T.; Yazawa, T. Study of Al_2O_3 effect on structural change and phase separation in Na_2O-B_2O_3-SiO_2 glass by NMR. *J. Mater. Sci.* **2000**, 35, 4865-4871.